European Journal of Medicinal Chemistry 124 (2016) 946–958

Contents lists available at ScienceDirect

European Journal of Medicinal Chemistry

journal homepage: http://www.elsevier.com/locate/ejmech

Research paper

Analogue based drug design, synthesis, molecular docking and anticancer evaluation of novel chromene sulfonamide hybrids as aromatase inhibitors and apoptosis enhancers

Mostafa M. Ghorab [a, b, *], Mansour S. Alsaid [a], Ghada H. Al-Ansary [c], Ghada A. Abdel-Latif [e], Dalal A. Abou El Ella [c, d]

[a] Department of Pharmacognosy, College of Pharmacy, King Saud University, P.O. Box 2457, 11451 Riyadh, Saudi Arabia
[b] Department of Drug Radiation Research, National Center for Radiation Research and Technology, Nasr City, 113701 Cairo, Egypt
[c] Department of Pharmaceutical Chemistry, Faculty of Pharmacy, Ain Shams University, 11566 Cairo, Egypt
[d] Department of Pharmaceutical Chemistry, Faculty of Pharmacy, Nahda University, 62511 Beni Suef, Egypt
[e] Department of Pharmacology, Faculty of Pharmacy, Misr International University, Cairo, Egypt

ARTICLE INFO

Article history:
Received 25 August 2016
Received in revised form
10 October 2016
Accepted 12 October 2016
Available online 13 October 2016

Keywords:
Sulfonamides
Chromene
Aromatase inhibitors
Apoptosis
Breast cancer

ABSTRACT

Twenty novel chromene derivatives carrying different sulfonamide moieties (**3**–**22**) were designed and synthesized. All the newly prepared compounds were evaluated for their *in vitro* anticancer activity against breast cancer cell line (T47D). Most of the synthesized compounds showed good to moderate activity (IC_{50} = 8.8–108.9 μM), where compound **16** (IC_{50} = 8.8 μM) exhibited higher activity compared to doxorubicin (IC_{50} = 9.8 μM). In order to determine the mechanism of the anticancer activity in T47D cells, the effect of the most potent compounds (**5**–**8**, **11**–**14**, and **16**–**18**) on the aromatase activity was tested. Most of the selected compounds showed significant inhibitory effect on the aromatase activity, with compound **18** showing IC_{50} = 4.66 μM. Furthermore, apoptosis studies were conducted on two of the most potent compounds (**8** & **16**) to estimate the proapoptotic potential of our compounds. Both induced the levels of active caspase 3, caspase 8 and caspase 9. Moreover, they surprisingly boosted the Bax/Bcl2 ratio 5936 & 33,000 folds, respectively compared to the control. Moreover, they showed mild cytotoxic effect (IC_{50} = 183.8 μM & 172.04 μM, respectively) in normal breast cells 184A1. Finally, a molecular docking study was performed to investigate the probable interaction with the aromatase enzyme.

1. Introduction

Breast cancer is one of the majority distinguished commonly spread cancer among women in different age groups [1]. It was categorized as the second leading cause of mortality among women. This tumor is illustrated by excess production of estrogen receptors for endogenous estrogens which is equally expressed in pre and postmenopausal breast tissue [2,3]. This accounts for the pathological effects of estrogens triggering cancer cell proliferation. As a matter of fact, intratumoral local estrogen production is controlled by the aromatase enzyme (CYP19), a member of the cytochrome P450 which controls *in situ* aromatization of C19 androgens to C18 estrogens [4,5]. Thus, one of the lucrative therapeutic approaches of treating estrogen-dependent breast cancer is the inhibition of bioconversion of androgens to estrogens by aromatase inhibitors (AIs) as a safer alternative to blockade of estrogen receptors by estrogen receptor antagonists (ERAs) [4–6].

AIs are comprised of two major classes on basis of their structural chemotype; namely steroidal and non-steroidal AIs. By virtue of their fewer incidence of side effects due to lack of estrogenic activity on the uterus and vasculature, non-steroidal AIs are gaining much popularity over the past few decades [6,7].

Recently, Pingaew et al. reported the synthesis of 1, 4-disubstituted-1, 2, 3-triazole derivatives bearing sulfonamide moiety (Fig. 1) which showed significant anti-proliferative activity [10]. This was proved by evaluating their aromatase inhibitory activity [10]. Interestingly, many of the tested sulfonamides exhibited marked aromatase inhibitory activity (IC_{50} = 0.2–9.4 μM).

* Corresponding author.Department of Pharmacognosy, College of Pharmacy, King Saud University, P.O. Box 2457, 11451 Riyadh, Saudi Arabia.
E-mail address: mmsghorab@yahoo.com (M.M. Ghorab).

http://dx.doi.org/10.1016/j.ejmech.2016.10.020
0223-5234/

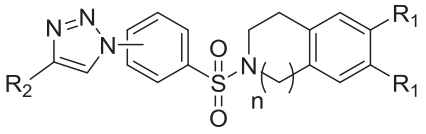

R_1 = H, OMe
R_2 = Ph, -CH_2-OPh
n= 0,1

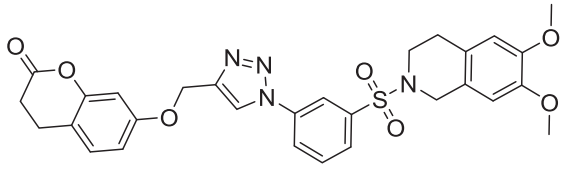

Lead compound (A)

Fig. 1. Cytotoxic agents revealed by Pingaew et al. [7] and the most active compound (A) against the aromatase enzyme (IC_{50} = 0.2 μM).

Moreover, their molecular docking was adopted to explore their binding modes with the aromatase [10]. The results revealed that most of their active compounds could snugly bind to the aromatase through H-bonding and $\pi-\pi$ stacking without chelation of the heme iron. The most active compound (A) (IC_{50} = 0.2 μM) displayed H-bonding interactions with Met 374 which is suggested to be the essential amino acid residue for the inhibitory activity. This was supported by the fact that such amino acid participated in a water-mediated H-bonding that facilitates the interaction between the aromatase and the C3-keto oxygen of androstanedione (ASD) to undergo enolization; the first step involved in its conversion to estrogen. Compound (A) showed an IC_{50} of 0.2 μM against the aromatase enzyme, thus it represents a good platform for the design of novel non-steroidal AIs [10].

Accordingly, based on their SAR findings we designed a novel series of chromene derivatives carrying different sulfonamide moieties, the designing strategy of which is illustrated in Fig. 2. Our design strategy is three folds; i. tetrahydroisoquiniline ring (THIQ) of the compound (**A**) was replaced with different acyclic and heterocyclic amines aiming to retain hydrophobic interactions with the receptor, ii. The tetrazole ring was replaced with semi-rigid open chain linker, finally, iii. The privileged chromene moiety was preserved to attain proper hydrophobic interaction with CYP19. All of the newly synthesized compounds will be evaluated for their *in vitro* anticancer activity against breast cancer cell line (T47D). It has been reported that the aromatase enzyme is overexpressed in this cell line [11]. Moreover, the most potent molecules will be evaluated for inhibition of the aromatase enzyme. Aromatase inhibition in cancer cells triggers apoptosis which synergistically augments the anti-tumor effect [12]. Considering these literature findings, the apoptotic effect of two of the most potent compounds will be evaluated to trace the apoptotic potency of our compounds. Finally, molecular docking of the compounds with the aromatase enzyme will be performed to explore their binding mode in a proof-of-concept study.

2. Results and discussion

2.1. Chemistry

The aim of this work was to design and synthesize a novel series of benzenesulfonamide incorporating biologically active chromene moieties to evaluate their anticancer activity. Thus, interaction of 3-acetyl-2-*H*-chromen-2-one **1** with dimethylformamide dimethyl acetal (DMF-DMA) under reflux in dry xylene gave the strategic starting material (*E*)-3-(3-(dimethylamino)acryloyl)-2*H*-chromen-2-one **2**. Compound **2** can be represented by three isomeric structures (**2a**–**c**) (Scheme 1). Enaminone **2** was assigned an *E*-configuration based on its ^{1}H-NMR spectrum which exhibited that the coupling constant of the doublet signals for olefinic protons equals to 12.4 Hz correlated to *E*-isomers. The behavior of enaminone **2** towards sulfa-drugs and dapsone was investigated. Thus, when enaminone **2** was reacted with sulfa-drugs and/or dapsone in absolute ethanol and glacial acetic acid (2:1), the corresponding chromene-sulfonamide derivatives **3**–**22** (Schemes 2 and 3) were obtained in good yield. The structures of the obtained compounds were established on the basis of microanalysis, IR, ^{1}H-NMR, ^{13}C-

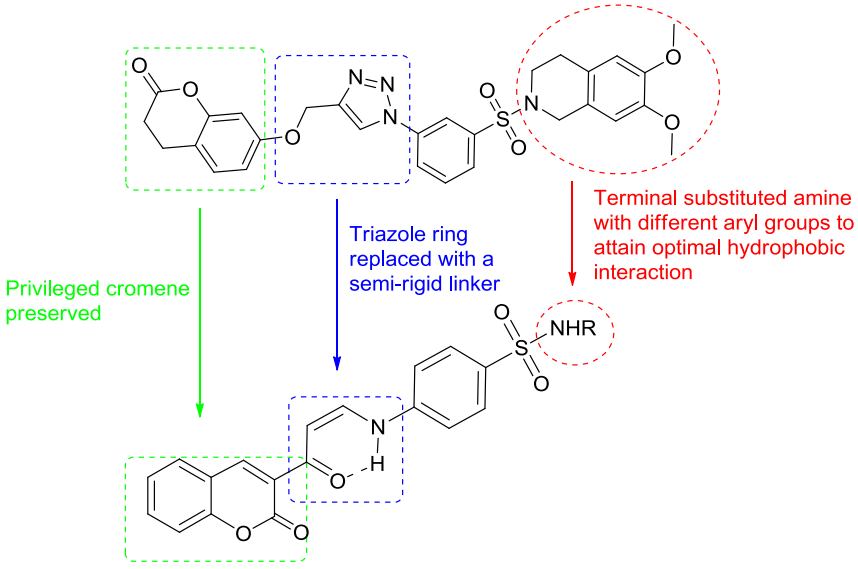

Fig. 2. Analogue-based design of chromene sulfonamide derivatives **3**–**20** as AIs.

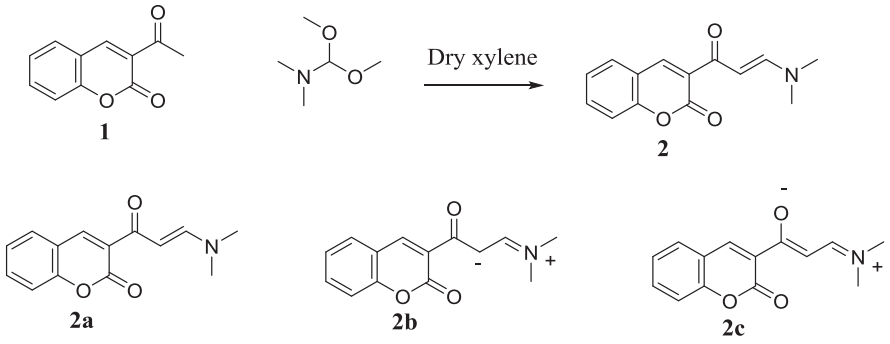

Scheme 1. Synthetic pathway for compound **2**.

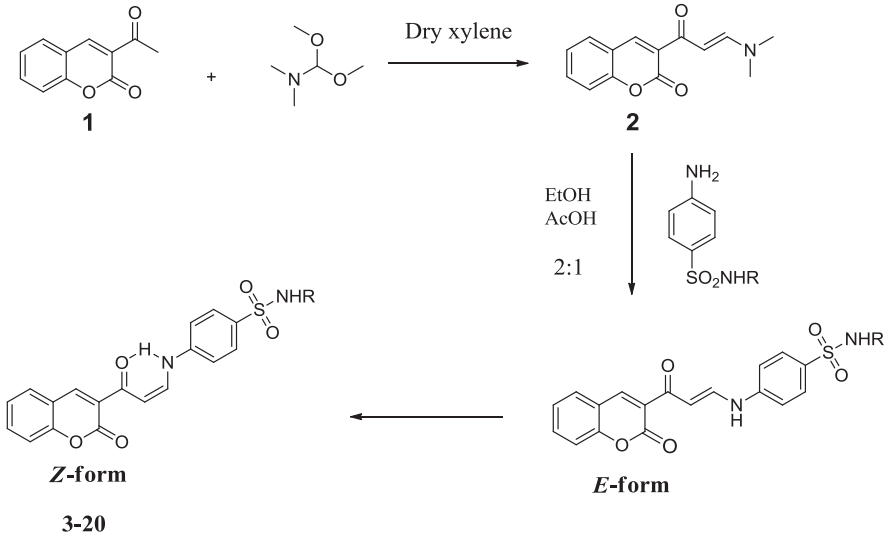

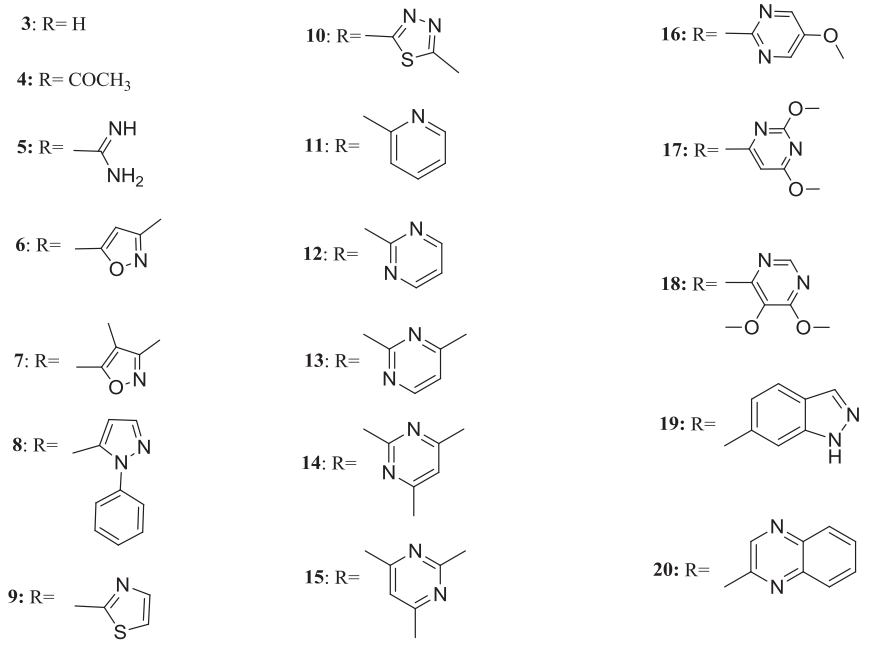

Scheme 2. Synthetic pathways for compounds **3**–**20**.

NMR and mass spectral data. IR of **3**–**20** indicated the presence of characteristic bands for NH, NH_2, SO_2 and two (CO) groups. The IR of **21** revealed the presence of characteristic bands for NH, SO_2 and two (CO) groups, while IR of **22** showed bands for NH, SO_2 and four (CO) groups. ^{1}H-NMR of **3**–**22** established that these structures are in (*Z*-form) not in (*E*-form), while the coupling constant of the doublet signals for olefinic protons is in the range of 8.4–8.6 Hz. Also, *Z*-form is stabilized by intramolecular hydrogen bonding

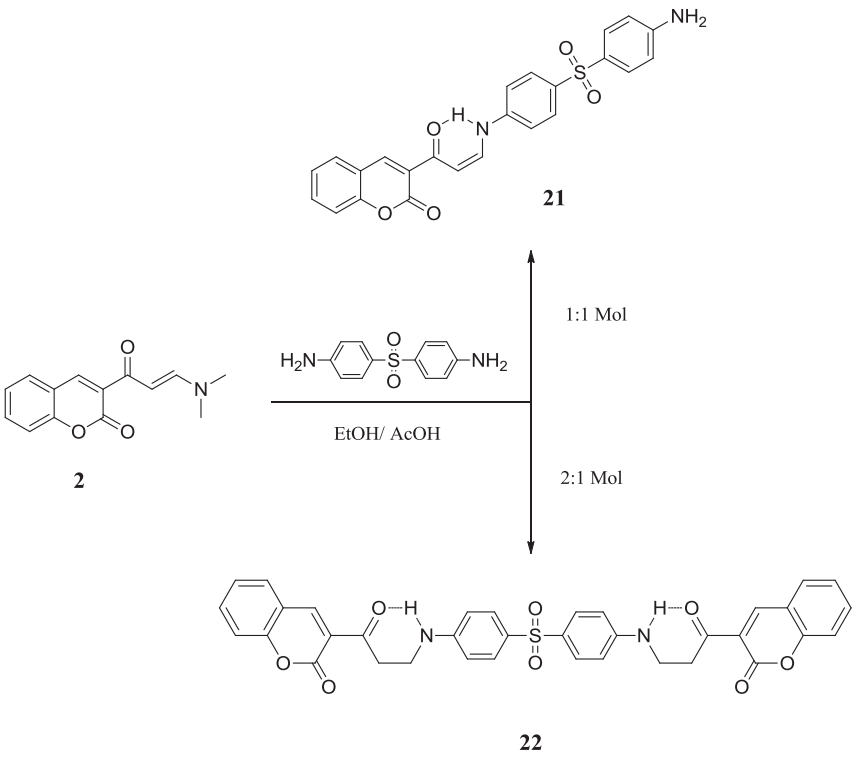

Scheme 3. Synthetic pathways of compounds **21** and **22.**

(Schemes 2 and 3). ^{1}H-NMR of **3** revealed signals at 8.6 ppm assigned to CH chromene, 10.5 ppm attributed to SO_2NH_2, 12.0 ppm due to NH group. ^{13}C-NMR of **3** showed signals at 158.9 and 184.4 ppm for two (CO) groups. IR of **4** showed bands at 1720, 1696 and 1660 cm^{-1} for three (CO) groups. ^{1}H-NMR of **4** revealed signals at 1.9 ppm for ($COCH_3$), 8.6 ppm assigned to CH chromene, 10.4 ppm attributed to SO_2NH and 12.0 ppm due to NH groups. ^{13}C-NMR of **4** showed signals at 159.3, 172.5 and 182.4 cm^{-1} for three (CO) groups. ^{1}H-NMR of **5** showed signals at 8.6 ppm for NH_2, 8.9 ppm assigned to CH chromene, 12.0 ppm due to NH group. ^{13}C-NMR of **5** showed signals at 158.4 ppm for imino group, 159.3 and 185.2 cm^{-1} for two (CO) groups. ^{1}H-NMR of **6** exhibited signals at 2.3 ppm for CH_3, 6.2 ppm for CH isoxazole, 8.6 ppm assigned to CH chromene, 12.0 ppm due to NH group. ^{13}C-NMR of **6** showed signals at 12.5 ppm for CH_3, 170.9 and 184.6 cm^{-1} for two (CO) groups. ^{1}H-NMR of **7** revealed signals at 2.0 and 2.1 ppm for two CH_3 groups, 8.7 ppm due to CH chromene, 12.0 ppm for NH group. ^{13}C-NMR of **7** exhibited signals at 6.2 and 10.7 ppm for two CH_3 groups, 172.4 and 185.7 ppm for two (CO) groups. ^{1}H-NMR of **10** showed signals at 2.6 ppm for CH_3, 8.7 ppm for CH chromene, 12.0 ppm for NH group. ^{13}C-NMR of **10** revealed signals at 16.4 ppm for CH_3, 168.2, 184.6 ppm for two (CO) groups. ^{1}H-NMR of **13** exhibited signals at 2.3 ppm for CH_3, 8.7 ppm for CH chromene, 12.0 ppm for NH group. ^{13}C-NMR of **13** showed signals at 23.8 ppm for CH_3, 172.5 ppm for two (CO) groups. ^{1}H-NMR of **14** exhibited signals at 2.2 ppm for two CH_3 groups, 8.5 ppm for CH chromene, 12.0 ppm for NH group. ^{13}C-NMR of **14** exhibited signals at 21.5 ppm for two CH_3 groups, 172.5 ppm for two (CO) groups. ^{1}H-NMR of **15** showed signals at 2.2, 2.3 ppm for two CH_3 groups, 8.7 ppm for CH chromene, 12.0 ppm for NH group. ^{13}C-NMR of **15** revealed signals at 19.0 and 21.5 ppm for two CH_3 groups, 166.7 and 172.5 ppm for two (CO) groups. ^{1}H-NMR of **16** exhibited signals at 3.8 ppm for OCH_3, 8.6 ppm for CH chromene, 12.0 ppm for NH group. ^{13}C-NMR of **16** showed signals at 56.7 ppm for (OCH_3) group, 159.3 and 172.5 ppm for two (CO) groups. ^{1}H-NMR of **17** showed signals at 3.77 and 3.79 ppm for two (OCH_3) groups, 8.7 ppm for CH chromene, 11.9 ppm for NH group. ^{13}C-NMR of **17** revealed signals at 55.0, 56.5 ppm for two (OCH_3) groups, 172.5 and 192.5 ppm for two (CO) groups. ^{1}H-NMR of **18** revealed signals at 3.7, 3.9 ppm for two (OCH_3) groups, 8.6 ppm for CH chromene, 12.0 ppm for NH group. ^{13}C-NMR of **18** exhibited signals at 54.4, 60.6 ppm for two (OCH_3) groups, 162.0, 184.6 ppm for two (CO) groups. ^{1}H-NMR of **19** showed signals at 8.1 ppm for CH indazole, 8.5 ppm for CH chromene, 11.9 ppm for NH, 12.9 ppm for NH indazole. ^{13}C-NMR of **19** exhibited signals at 158.9 and 185.5 ppm for two (CO) groups. On the other hand, interaction of compound **2** with dapsone in molar ratio (1:1 mol) the corresponding mono compound **21** was formed, while the bis-compound **22** was obtained under the same condition but in molar ratio (2:1 mol) (Scheme 3). The structures of **21** and **22** were confirmed on the basis of elemental analyses, IR, ^{1}H-NMR, and ^{13}C-NMR data. IR of **21** showed characteristic bands at 3431, 3413, 3396 cm^{-1} (NH_2, NH), 1718, 1654 cm^{-1} two (CO) groups, 1363, 1181 cm^{-1} (SO_2). ^{1}H-NMR of **21** revealed signals at 6.2 ppm for NH_2, 8.6 ppm CH chromene, 10.8 ppm for NH group. ^{13}C-NMR of **21** exhibited signals at 159.6 and 172.4 ppm for two (CO) groups. IR of **22** showed characteristic bands at 3421 and 3366 cm^{-1} (NH), 1718 and 1636 cm^{-1} for two (CO) groups, 1361 and 1181 cm^{-1} for (SO_2). ^{1}H-NMR of **22** revealed signal at 8.7 ppm for two CH chromene, 10.9 ppm for two NH groups. ^{13}C-NMR of **22** exhibited signals at 159.6 and 172.5 ppm for four (CO) groups.

2.2. Biological evaluation

2.2.1. In vitro cytotoxic activity

Our biological evaluation journey started by evaluating the *in vitro* anticancer activity of the synthesized series of chromene derivatives bearing functional sulfonamide moieties **(2–22)** against breast cancer cell line (T47D) (Table 1). Doxorubicin (CAS 23214-92-

8) was taken as the reference drug for its well-known clinical utility in managing a wide range of tumors. All the tested chromenes exerted gradual cellular log kill with an IC_{50} values ranging from 146.5 μM to 8.8 μM except for compounds **4** and **9** which did not show any activity relative to doxorubicin under the experiment conditions in T47D cells. Introduction of a sulfonamide moiety resulted in significant increase in activity as compound **2** (IC_{50} = 146.5 μM) bearing a terminal tertiary amine is compared with compound **3** (IC_{50} = 108 μM) that possesses a terminal unsubstituted sulfonamide. This marked drop in IC_{50} value suggests that a terminal sulfonamide group plays crucial role in the anticancer activity.

Results showed that sulfonamide substituents having terminal phenyl pyrazolyl, pyridyl, methyl substituted pyrimidinyl and methoxy substituted pyrimidinyl possess significant antiproliferative activity suggesting that the aforementioned pharmacophores play crucial roles in manifesting anticancer activity. Having a thorough investigation of the results, it could be deduced that a terminal methoxy or dimethoxy substituted pyrimidinyl group markedly enhances the activity as compounds **16**, **17** and **18** showed IC_{50} values ranging from 37 μM and going down to 8.8 μM. Among them compound **16** exerted the highest activity having IC_{50} value of 8.8 μM which is more potent than that of the reference drug doxorubucin itself, whereas compound **18** had an IC_{50} of 9.8 μM that is comparable to that of doxorubicin. This finding is coherent with previous conclusions made by Pingaew et al. [7] and suggests that methoxy substituted pyrimidinyl groups are good pharmacophoric moeities for anticancer activity.

On the other hand, compounds bearing a terminal five membered heterocyclic rings showed low to moderate cytotoxicity with IC_{50} values ranging from 68.4 μM to 94 μM with the exception of compound **9** which bears an unsubstituted thiazolyl ring and showed no antiproliferative activity compared to doxorubicin. Among these compounds, compound **7** that bears a dimethyl isoxazolyl ring (IC_{50} = 68.4 μM) showed slight higher activity than its methyl isoxazolyl analogue **6** (IC_{50} = 75.6 μM). Compound **10** (IC_{50} = 94 μM) bearing a methyl thiadiazolyl group showed much lower activity which suggests that the thiadiazolyl group is not a good candidate for future work.

Analyzing the IC_{50} values of the compounds, it is noticed that those having a terminal six membered heterocylce moiety namely compounds **11**–**18** (IC_{50} values ranging from 8.8 μM to 62 μM) showed better activity than those bearing a terminal five membered heterocyle namely compounds **6**–**10** (IC_{50} values ranging from 68.4 μM to 94 μM) with the exception of compound **9** bearing an unsubstituted thiazolyl ring that showed no inhibitory activity and compound **8** which has a terminal phenyl pyrazolyl group and showed marked potency with IC_{50} value of 9.2 μM which is comparable to that of doxorubicin.

Moreover, compounds **19** (IC_{50} = 96 μM) and **20** (IC_{50} = 86 μM) that possess a fused bicyclic ring showed lowest activities. This can be accounted for by the bulkiness of the large hydrophobic groups that hinders snuggle binding to the target enzyme.

Promisingly, *p*-methoxypyrimidinyl analogue **16** (IC_{50} = 8.8 μM) proved to be the most potent compound that manifested superior antiproliferative activity to doxorubicin (IC_{50} = 9.8 μM) against T47D cell line. Surprisingly, the same result was observed for compound **8** bearing a phenyl thiazolyl moeity (IC_{50} = 9.2 μM) which suggests that both compounds are good platform for further optimization to develop potent anticancer agents.

2.2.2. Evaluation of aromatase inhibitory activity

Gaining insight into the antiproliferative activity against breast cancer cell line T47D of our novel series of chromene derivatives (**3**–**22**), eleven of the most potent compounds (**5, 6, 7, 8, 11, 12, 13, 14, 16, 17** and **18**) were further chosen to be evaluated for their aromatase inhibitory activity in an attempt to explore their probable mode of action. Their percentage inhibition was determined and the IC_{50} values for the compounds that exhibited percentage inhibition above 50% (**8, 11, 13, 16** and **18**) were recorded that indicate the dose that prevents the proliferation of half of the population (Table 1, Fig. 3). Letrozole; a well-known FDA approved AI, was taken as the reference drug.

Results showed that most of the tested compounds have moderate to high aromatase inhibitory activity ranging from 20% to 81% and their IC_{50} values varied from 12.5 μM down to 4.66 μM. Five of our compounds (**8, 11, 13, 16 & 18**) showed higher percentage inhibition of the aromatase enzyme compared to letrozole (70%, 65%, 67%, 81%, 69% & 58%) where all of them exhibited higher potencies relative to the reference drug (IC_{50} values 5.089 μM, 12.53 μM, 9.52 μM, 6.07 μM, 4.66 μM vs 29.5 μM for letrozole) where compound **16** bearing a terminal methoxypyrimidinyl group showed

Table 1
Biological evaluation of the newly synthesized compounds **2**–**22**.

Compound No.	IC_{50} against T47D (μM)	% inhibition of aromatase enzyme	IC_{50} of aromatase enzyme (μM)
2	146.5	–	–
3	108.9	–	–
4	NA	–	–
5	87.6	30	–
6	75.6	28	–
7	68.4	20	–
8	9.2	70	5.089
9	–	–	–
10	94.0		–
11	37.6	65	12.53
12	75.2	41	–
13	24.5	67	9.52
14	62.2	30	–
15	100.0	–	–
16	8.8	81	6.07
17	37.8	44	–
18	9.8	69	4.66
19	96.5	–	–
20	86.9	–	–
21	91.9	–	–
22	70.3	–	–
Doxorubicin	9.8	–	–
Letrozole	–	58	29.50

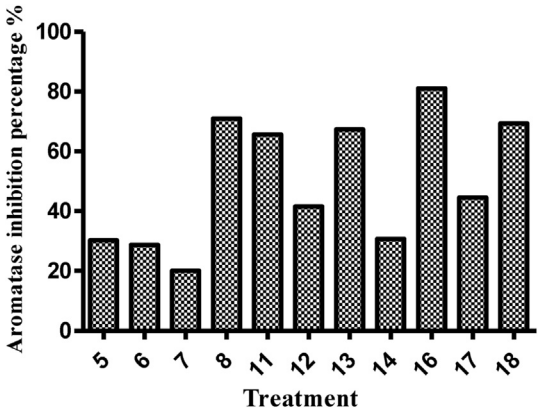

Fig. 3. The effect of the synthesized compounds (**5**–**8**, **11**–**14**, and **16**–**18**) on aromatase activity.

the highest aromatase inhibitory activity (81%) while compound **18** bearing a terminal dimethoxypyrimidinyl moiety showed the lowest IC_{50} value (4.66 μM). Scrutinizing the aromatase inhibitory results reveals that the compounds bearing terminal six membered heterocycle moiety (**11**–**14** and **16**–**18**) showed better aromatase inhibitory activity (30%–81%) than those bearing terminal five membered heterocycle (**5**–**8**) which showed lower aromatase inhibitory activity ranging from 20% to 30% with the exception of compound **8** bearing a phenyl pyrazolyl group showing 70% inhibition and an IC_{50} value of 5.089 μM (Fig. 3).

These deduced SAR results are again coherent with the previous SAR results observed in the T47D cell line analysis, suggesting that the presence of a terminal lipophilic six membered heterocycle or alternatively a bulky lipophilic phenylpyrazolyl group favors the aromatase inhibitory activity and consequently improved antiproliferative activity against breast cancer cells.

2.3. Apoptosis studies

Apoptosis is a programmed routine by which cells signal their own termination. This "self-automated" death is critical for maintenance of cellular homeostasis that conserves its integrity [13]. For cancer cells to proliferate and divide unconditionally, they cunningly "switch off" apoptosis. Thus, induction of apoptosis serves as a logic tactic for tumor suppression [14].

From literature survey, we came to know that inhibition of the aromatase enzyme leads consequently to induction of apoptosis [12]. Since our targeted compounds proved to have significant aromatase inhibitory activity, we were endeavored to explore their ability to induce the apoptosis cascade. Herein, two of the most potent compounds against T47D cell line (compounds **8** & **16**, IC_{50} = 9.2 μM & 8.8 μM, respectively) were selected as a representative molecules to conduct apoptosis studies in an attempt to reveal the proapoptotic potential of our synthesized chromenesulfonamide derivatives.

2.3.1. Effects on activation of proteolytic caspases cascade

The crucial mediators of apoptosis comprise a family of cysteineaspartic proteases known as caspases [15]. Their activation plays a pivotal role in the programmed cell death or apoptosis. Accordingly, the effects of compounds **8** & **16** on caspase 3 were evaluated and compared to that of letrozole as a reference drug, in order to trace their apoptotic effect and then their effects on caspases 8 & 9 were measured in order to gain insight whether they induce apoptosis through the intrinsic or the extrinsic pathway or through induction of both apoptotic pathways (Fig. 4). Our results showed that compounds **8** & **16** markedly increased the level of active caspase 3 by 45 & 20.6 folds, respectively compared to control cells. This implies that compound **8** induced caspase 3 approximately three times compared to letrozole whereas compound **16** produced a 1.3 fold increase in caspase 3 induction Furthermore, both compounds **8** & **16** produced a significant increase in caspase 8 by 40 & 21.75 folds, respectively, and to a lesser extent caspase 9 was also increased by almost 10 & 9.91 folds, respectively, compared to the control (Fig. 4). These results suggest that these compounds may have activated both intrinsic and extrinsic pathways of apoptosis.

2.3.2. Effects on mitochondrial apoptosis pathway (Bcl-2 family) proteins

Mitochondrial apoptotic pathway is chiefly regulated by the members of the Bcl-2 family [16]. Among these, Bcl2 and Bax finely tune this programmed process. The Bcl2 protein inhibits apoptosis (anti-apoptotic) while Bax stimulates it (pro-apoptotic). Thus, the balance between these two different opposing proteins regulates the cell fate [17,18]. Increments in the Bax/Bcl2 ratio trigger the release of mitochondrial cytochrome C into the cytosol which in turn potentiates a cascade of caspases that ultimately leads to activation of caspase 3; the apoptosis executioner [19,20]. In this study, T47D cells were treated with the IC_{50} of compounds **8** & **16** and their effect on the expression levels of Bcl2, Bcl-xl and Bax were determined as illustrated in Table 2.

As shown by the results, compounds **8** & **16** boosted the level of the pro-apoptotic protein; Bax by approximately 16,000 folds and 7190 folds, respectively. Moreover, compound **8** markedly reduced the levels of the anti-apoptotic proteins Bcl2 and Bcl-xl by approximately 369 folds and 1965 folds, respectively compared to the control, while compound **16** produced a 819.65 folds decrease in Bcl2 and a 111.35 folds reduction in Bcl-xl levels in comparison to the control.

A rather more indicative and precise value for apoptosis induction is the Bax/Bcl2 ratio as it gives a more accurate estimation of the overall proapoptotic activity of the molecule. Analyzing the results reveals that compounds **8** & **16** interestingly boosted the Bax/Bcl2 ratio by approximately 33,000 folds and 5936 folds, respectively, as compared to the control. Collectively, these findings that both compounds markedly increased Bax level, downregulated Bcl2 and Bcl-xl levels, concomitantly with tremendously augmenting the Bax/Bcl2 ratio proved undoubtedly their pro-apoptotic effect.

2.3.3. Cell cycle analysis

In general, anticancer agents abort the growth and proliferation of cancerous cells by arresting cell division at various checkpoints [21]. Treatment of the cancer cells with potent anticancer agents unravel the distinguish cells in various phases of the cell cycle. In the current study, T47D cells were treated with compound **8** at its IC_{50} (9.2 μM). The obtained data (Fig. 5) obviously indicate that compound **8** arrested the cell cycle at G2/M phase when compared to untreated control (44.5% and 15.81%, respectively). Parallel to these findings, the cell population in G1 and S phases markedly decrease after treatment (9.2% and 14.6% vs 64.92% and 17.14%, respectively). These results reveal that in T47D cells, cell cycle arrest in the G2/M phase contributes to the compound cytotoxicity.

2.3.4. Cytotoxicity test

The cytotoxic effects of compound **8** & **16** were tested on normal breast cells 184A1 using SRB assay (Skehan et al.) [22]. Both compounds showed mild cytotoxic effect with an IC_{50} of 183.8 μM & 172.04 μM, respectively (Fig. 6). This result indicates the selectivity of compounds **8** & **16** for tumor breast cancer cells and their relative safety for normal breast cells.

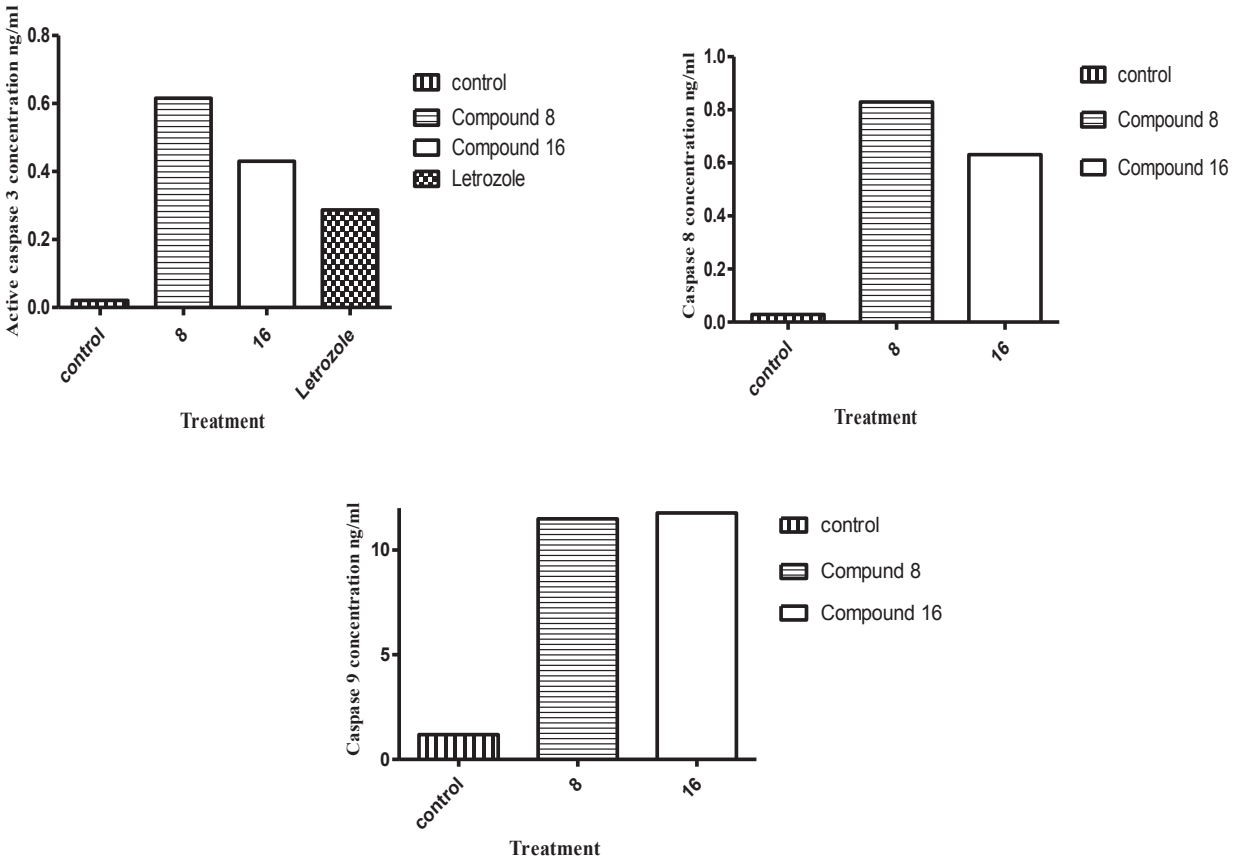

Fig. 4. The effect of compounds **8** & **16** on the active caspases; 3, 8 & 9 in T47D cells.

Table 2
Effect of compound **8** & **16** on the genes expression of some apoptosis key markers.

Compound No.	BAX (IU/mL)	BCL2 (IU/mL)	BCL-xL (IU/mL)
8	402,127	1540	384
16	176,887	693	6776
Control	24.6	568,019	754,565

3. Molecular docking

Molecular docking of chromene derivatives (**3**–**22**) to the aromatase enzyme was performed to investigate their binding interactions and to explore their binding modes. Moreover, our lead compound was also docked in order to investigate its binding pattern to the aromatase active site.

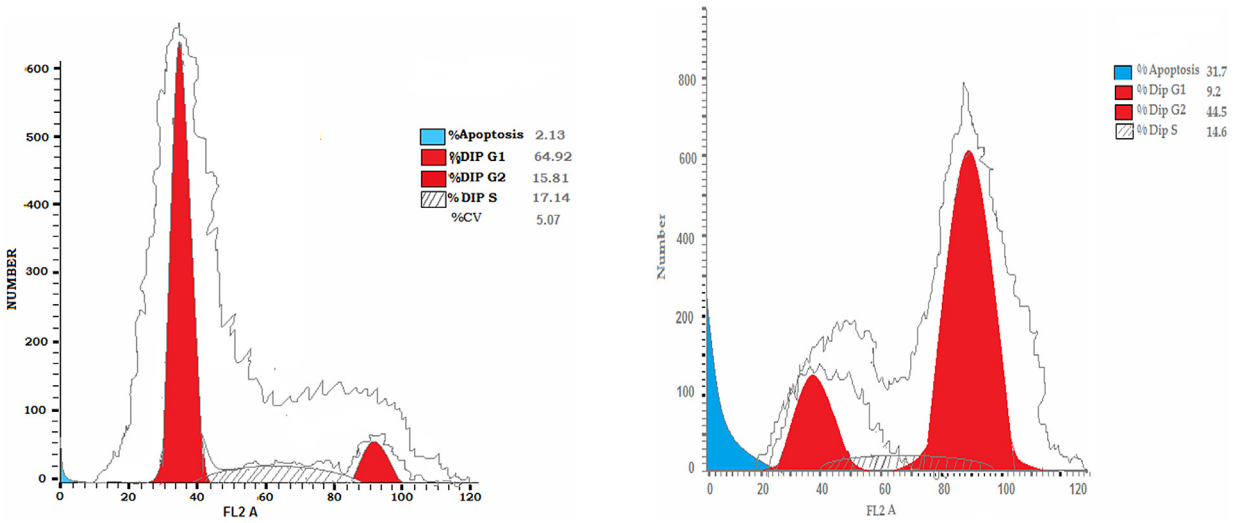

Fig. 5. Effect of compound **8** on the phases of the cell cycle in T47D cells.

The interaction of the co-crystallized natural substrate androstanedione (ADS) (Fig. 7) displayed hydrogen bonding of the CO group at position 17 with the amino group of the key amino acid Met374 which is well known to initiate the enzymatic oxidation cascade. Moreover, the steroidal backbone forms hydrophobic interaction with amino acid residues (i.e. Ile133, Trp224 and Leu477).

Our lead compound shows good interaction CDOCKER score (−44.51913 Kcal/mol). Scrutinizing its binding mode disclosed that the oxygen of the sulfonamide group formed 2 significant H-bonds with the key amino acid Met 374 and anchoring the compound into the active pocket (Fig. 8). Meanwhile the compound interacts with a hydrophobic site (Trp 224, Val 370 and Ala306) through its coumarinyl moiety.

By analyzing the binding pattern between the most active compound (**18**) and the aromatase enzyme and investigating the interaction energy, thoroughly investigating the binding patterns of the ligand reveals that it was able to form H-bonds and hydrophobic interactions with the amino acid residues in the active site with excellent CDOCKER interaction energy score (−58.7918 Kcal/mol) which is superior to the lead compound CDOCKER score (−44.51913 Kcal/mol). Compound **18** forms two significant H-bonds between the sulfonyl oxygen and the key amino acid Met 374 (2.32 Å) and the amino acid Arg 115 (2.5 Å) while its coumarinyl moiety fits into a hydrophobic pocket (Cys 437, Ala 307 and Ala306) while its methoxyprimidinyl group forms hydrophobic interactions with another hydrophobic pocket (Leu 477, Val 370 and Trp 224) (Figs. 8 and 9).

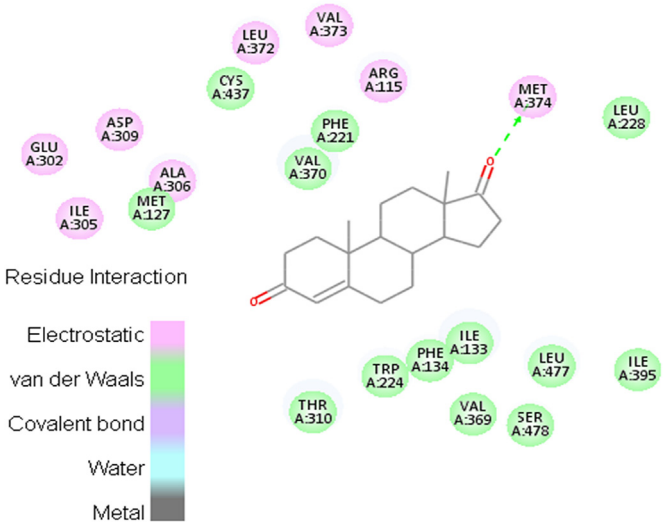

Fig. 7. 2D diagram of ASD with the aromatase.

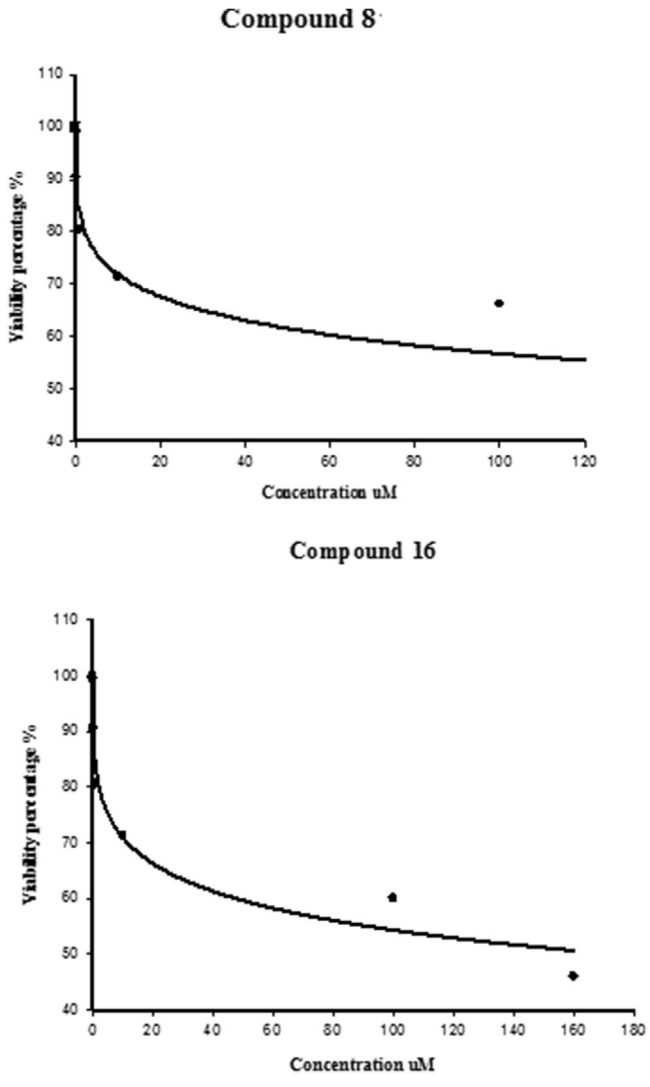

Fig. 6. The effect of compounds **8** & **16** on the viability percentage of 184A1 normal breast cells.

4. Conclusion

In summary, we designed and synthesized a novel series of chromene derivatives bearing sulfonamide moieties based on structural diversification of a lead compound (**A**) revealed by Pingaew et al. in 2015 that proved to have potent aromatase inhibitory activity (IC_{50} = 0.2 μM). The antiproliferative activities of the synthesized compounds was evaluated against T47D cell line where most of the targeted compounds showed moderate to excellent antiproliferative activities with IC_{50} values ranging from 108.9 μM down to 8.8 μM. Further investigation of their expected mode of action directed us to estimate their ability to inhibit the aromatase enzyme and thus suppress breast cancer growth. Eleven of the most potent compounds against the T47D cell line were chosen for this study. Results revealed that all the tested compounds were able to inhibit the aromatase activity in considerable ratios ranging from 20% up to 81% inhibition where five compounds showed superior inhibitory potency to letrozole. This clearly demonstrates that these compounds suppress breast cancer proliferation through inhibition of CYP19. Endeavored by the previous findings and inlighted by literature search that directly correlates aromatase inhibition to apoptosis induction [8,9], we further conducted apoptosis studies to estimate the proapoptotic potential of our compounds. Two of the most potent compounds on T47D (**8** & **16**, IC_{50} = 9.2 μM & 8.8 μM, respectively) were chosen for further apoptosis studies. Compounds **8** & **16** boosted the Bax/Bcl2 ratio, they also markedly induced the levels of caspase 3, caspase 8 and caspase 9 as previously discussed.

To our knowledge, cytotoxic compounds exert their antiproliferative activity either by apoptosis induction or by arresting the cell cycle at definite checkpoints or a combination effect of both apoptosis induction and cell cycle block. Thus, we studied the effect of compound **8** on the cell cycle in the aim of fully profiling the antiproliferative activity of our compounds. Scruitinizing the cell cycle analysis results revealed that compound **8** arrests cell proliferation in the G2/M phase.

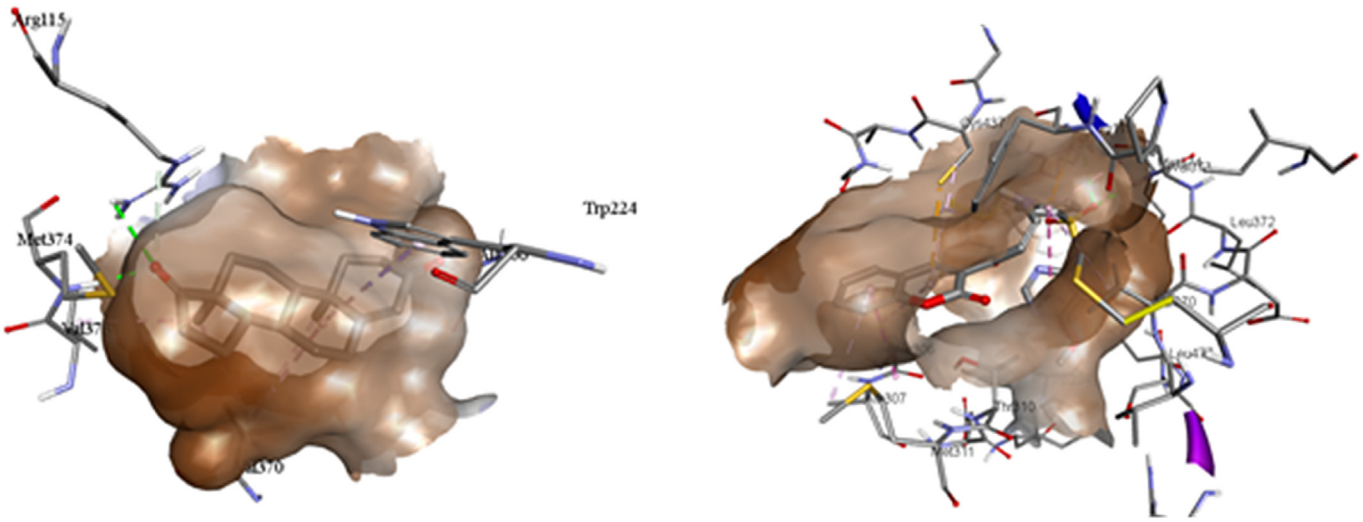

Fig. 8. Binding modes of lead compound (to the left) and of compound **18** (to the right). Both compounds show two H-bonds with Met374 and Arg 115, also hydrophobic interactions between the coumarinyl moiety and amino acids Cys 437, Ala 307 and Ala 306 in addition to hydrophobic interaction between the dimethoxypyrimidinyl group and amino acids Leu 477, Val 370 and Trp 224 (Hydrophobic pocket color is ranging from brown to blue according to degree of hydrophobicity). (For interpretation of the references to colour in this figure legend, the reader is referred to the web version of this article.)

Induction of the mitochondrial apoptotic protein Bax, together with downregulation of the antiapoptotic proteins Bcl2 and Bcl-xl, synchronized with the induction of both caspase 8 and caspase 9 and the ultimate induction of the executioner caspase 3 proved that our compounds exert their apoptotic effect through triggering both the mitochondrial-intrinsic pathway and the receptor-mediated extrinsic pathway. These findings were coherent with our earlier results that our compounds have potential aromatase inhibitory activities.

Further molecular docking studies were conducted in order to explore the binding modes and possible interactions with the target enzyme. Molecular docking studies revealed that most of the sulfonamide series could snugly fit into the aromatase active site with low interaction energies. Moreover, most of the investigated compounds were able to form H-bonds with the key amino acid Met 374.

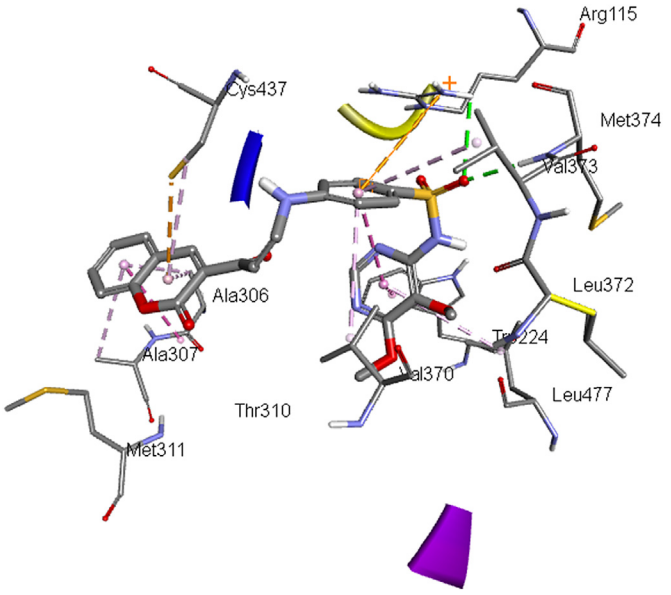

Fig. 9. 3D diagram of the interaction of compound **18** in the active site of the aromatase enzyme (PDB: 3EQM) showing two hydrogen bonds with Met 374 and Arg 115. Atoms are coloured by atom type and hydrogen bonds are represented by green dots. (For interpretation of the references to colour in this figure legend, the reader is referred to the web version of this article.)

5. Experimental

5.1. Chemistry

Melting points (uncorrected) were and determined in open capillary on a Gallen Kamp melting point apparatus (Sanyo Gallen Kamp, UK). Precoated silica gel plates (*Kieselgel* 0.25 mm, 60 F254, Merck, Germany) were used for thin layer chromatography. A developing solvent system of chloroform/methanol (8:2) was used and the spots were detected by ultraviolet light. IR spectra (KBr disc) were recorded using an FT-IR spectrophotometer (Perkin Elmer, USA). ^{1}H-NMR spectra were scanned on a NMR spectrophotometer (Bruker AXS Inc., Switzerland), operating at 500 MHz for ^{1}H and 125.76 MHz for ^{13}C. Chemical shifts are expressed in δ-values (ppm) relative to TMS as an internal standard, using DMSO-d_6 as a solvent. Elemental analyses were done on a model 2400 CHNSO analyser (Perkin Elmer, USA). All the values were within ±0.4% of the theoretical values. Electron impact Mass Spectra were recorded on a, Shimadzu Gc-Ms-Qp 5000 instruments (Shimadzu, Tokyo, Japan). All reagents used were of AR grads. The starting material 3-acetyl-2-*H*-chromen-2-one **1** was purchased from sigma (USA) and was directly used for the preparation of target compounds.

5.1.1. (E)-3-(3-dimethylamino) acryloyl)-2H-chromen-2-one **2**

To a solution of 3-acetyl-2-*H*-chromen-2-one **1** (1.88 g, 0.01 mol) in dimethylformamide-dimethylacetal (1. 19 g, 0.01 mol) in dry xylene (20 mL) was refluxed for 24 h the obtained solid while hot was collected by filtration and recrystallized from ethanol to give compound **2**.

Yield, 88%; m.p. 158.0 °C. IR: 3080 (arom.), 2997, 2931, 2839 (aliph.), 1718, 1635 (2CO). ^{1}H-NMR: 3.1 [s, 6H, N-$(CH_3)_2$], 6.0, 7.2 [2d, 2H, CH=CH, J = 12.4 Hz], 7.3–7.8 [m, 4H, Ar–H], 8.5 [s, 1H, CH chromene]. ^{13}C-NMR: 45.4 (2), 96.7, 116.3, 119.2, 125.0, 127.3, 130.1, 145.6, 154.3 (2), 159.2, 182.6. MS *m*/*z* (%): 243 (M^+) (15.29), 98 (100).

Anal. Calcd. for $C_{14}H_{13}NO_3$ (243.26): C, 69.12; H, 5.39; N, 5.76. Found: C, 69.47; H, 5.14; N, 5.53.

*5.1.2. Synthesis of chromene-sulfonamide derivatives (**3**–**20**)*

5.1.2.1. General procedure. A mixture of **2** (1.88 g, 0.01 mol) and sulfa-drugs (0.012 mol) in absolute ethanol (10 mL) and glacial acetic acid (5 mL) was refluxed for 21 h, then left to cool. The solid product formed was collected by filtration and recrystallized from ethanol-dimethylformamide to give **3–20.**

*5.1.2.1.1. (Z)-4-(3-Oxo-3-(2-oxo-2H-chromen-3-yl) prop-1-enylamino) benzenesulfonamide **3**.* Yield, 91%; m.p. 292.6 °C. IR: 3336, 3250 (NH_2, NH), 3095 (arom.), 1697, 1662 (2CO), 1355, 1166 (SO_2). ^{1}H-NMR: 6.5, 7.3 [2d, 2H, CH═CH, J = 8.4 Hz]. 7.4–8.5 [m, 8H, Ar–H], 8.6 [s, 1H, CH chromene], 10.5 [s, 2H, SO_2NH_2], 12.0 [s, 1H, NH]. ^{13}C-NMR: 98.2, 115.7 (2), 116.4, 119.1, 125.2, 126.5, 127.9, 128.0 (2), 130.8, 133.9, 143.1, 146.3, 154.6, 154.7, 158.9, 184.4. MS *m*/*z* (%): 370 (M^+) (8.28), 93 (100). Anal. Calcd. for $C_{18}H_{14}N_2O_5S$ (370.38): C, 58.37; H, 3.81; N, 7.56. Found: C, 58.08; H, 3.46; N, 7.82.

*5.1.2.1.2. (Z)-N-4-(3-Oxo-3-(2-oxo-2H-chromen-3-yl) prop-1-enylamino) phenylsulfonyl) acet-amide **4**.* Yield, 84%; m.p. 217.2 °C. IR: 3246 (NH), 3091 (arom.), 2974, 2873 (aliph.), 1720, 1682, 1660 (3CO), 1369, 1159 (SO_2). ^{1}H-NMR: 1.9 [s, 3H, $COCH_3$], 6.6, 7.3 [2d, 2H, CH═CH, J = 8.5 Hz]. 7.4–8.5 [m, 8H, Ar–H], 8.6 [s, 1H, CH chromene], 10.4 [s, 2H, SO_2NH], 12.0 [s, 1H, NH]. ^{13}C-NMR: 19.0, 94.8, 112.7 (2), 115.6, 116.4, 125.2, 126.8, 127.5, 128.7 (2), 130.1, 130.2, 144.8 (2), 154.6 (2), 159.3, 172.5, 182.4. MS *m*/*z* (%): 412 (M^+) (11.73), 93 (100). Anal. Calcd. for $C_{20}H_{16}N_2O_6S$ (412.42): C, 58.25; H, 3.91; N, 6.79. Found: C, 58.01; H, 3.56; N, 6.42.

*5.1.2.1.3. (Z)-N-Carbamimidoyl-4-(3-oxo-3-(2-oxo-2H-chromen-3-yl) prop-1-enylamino) benz-enesulfonamide **5**.* Yield, 89%; m.p. 301.8 °C. IR: 3433, 3329, 3232 (NH_2, NH), 3100 (arom.), 1719, 1708 (2CO), 1610 (CN), 1361, 1174 (SO_2). ^{1}H-NMR: 6.5, 7.2 [2d, 2H, CH═CH, J = 8.4 Hz]. 7.3–8.2 [m, 8H, Ar–H], 8.6 [s, 2H, NH_2], 8.9 [s, 1H, CH chromene], 10.4 [s, 2H, SO_2NH + NH imino], 12.0 [s, 1H, NH]. ^{13}C-NMR: 98.0, 112.8 (2), 115.6, 119.1, 125.2, 126.6, 127,8, 130.5 (2), 131.2, 133.9, 142.5, 146.7, 151.8, 154.6, 158.4, 159.3, 185.2. MS *m*/*z* (%): 412 (M^+) (3.54), 121 (100). Anal. Calcd. for $C_{19}H_{16}N_4O_5S$ (412.42): C, 55.33; H, 3.91; N, 13.58. Found: C, 55.64; H, 4.22; N, 13.90.

*5.1.2.1.4. (Z)-N-(3-Methylisoxazol-5-yl)-4-(3-oxo-3-(2-oxo-2H-chromen-3-yl) prop-1-enylami-no) benzenesulfonamide **6**.* Yield, 88%; m.p. 201.6 °C. IR: 3260, 3183 (NH), 3088 (arom.), 2895, 2839, (aliph.), 1722, 1683 (2CO), 1610 (CN), 1375, 1184 (SO_2). ^{1}H-NMR: 2.3 [s, 3H, CH_3], 6.2 [s, 1H, CH isoxazole], 6.5, 7.1 [2d, 2H, CH═CH, J = 8.4 Hz], 7.2–8.5 [m, 8H, Ar–H], 8.6 [s, 1H, CH chromene], 10.6 [s, 1H, SO_2NH], 12.0 [s, 1H, NH]. ^{13}C-NMR: 12.5, 95.7, 104.3, 113.1 (2), 115.9, 116.4, 124.6, 125.1, 126.4, 129.1, 130.8 (2), 132.4, 144.4, 145.5, 153.7, 154.6, 158.1, 159.3, 170.9, 184.6. MS *m*/*z* (%): 451 (M^+) (7.39), 97 (100). Anal. Calcd. for $C_{22}H_{17}N_3O_6S$ (451.45): C, 58.53; H, 3.80; N, 9.31. Found: C, 58.25; H, 3.47; N, 8.94.

*5.1.2.1.5. (Z)-N-(3,4-Dimethylisoxazol-5-yl)-4-(3-oxo-3-(2-oxo-2H-chromen-3-yl) prop-1-enyl-amino) benzenesulfonamide **7**.* Yield, 81%; m.p. 212.8 °C. IR: 3412, 3326 (NH), 3097 (arom.), 2946, 2886 (aliph.), 1718, 1654 (2CO), 1608 (CN), 1345, 1165 (SO_2). ^{1}H-NMR: 2.0, 2.1 [2s, 6H, $2CH_3$], 6.2, 6.7 [2d, 2H, CH═CH, J = 8.5 Hz]. 6.9–8.5 [m, 8H, Ar–H], 8.7 [s, 1H, CH chromene], 10.4 [s, 1H, SO_2NH], 12.0 [s, 1H, NH]. ^{13}C-NMR: 6.2, 10.7, 98.7, 104.7, 113.1 (2), 118.6 (2), 125.0, 127.6, 128.1, 128.3, 129.1 (2), 132.8, 142.6, 144.9, 153.8 (2), 161.6 (2), 172.4, 185.7. MS *m*/*z* (%): 465 (M^+) (4.87), 168 (100). Anal. Calcd. for $C_{23}H_{19}N_3O_6S$ (465.48): C, 59.35; H, 4.11; N, 9.03. Found: C, 59.11; H, 4.36; N, 9.34.

*5.1.2.1.6. (Z)-4-(3-Oxo-3-(2-oxo-2H-chromen-3-yl) prop-1-enylamino)-N-(thiazol-2-yl) benze-nesulfonamide **8**.* Yield, 79%; m.p. 284.5 °C. IR: 3391, 3283 (NH), 3102 (arom.), 2956, 2861 (aliph.), 1716, 1667 (2CO), 1607 (CN), 1366, 1183 (SO_2). ^{1}H-NMR: 6.5, 6.7 [2d, 2H, CH═CH, J = 8.4 Hz], 6.9–8.5 [m, 10H, Ar–H], 8.6 [s, 1H, CH chromene], 10.6 [s, 1H, SO_2NH], 12.0 [s, 1H, NH]. ^{13}C-NMR: 98.3, 108.6, 112.9 (2), 115.7, 119.1, 124.9, 125.2, 126.5, 128.2, 130.5 (2), 133.9, 137.3, 143.3, 146.8, 154.6, 154.7, 159.3, 169.0, 185.4. MS *m*/*z* (%): 453 (M^+) (33.42), 101 (100). Anal. Calcd. for $C_{21}H_{15}N_3O_5S_2$ (453.49): C, 55.62; H, 3.33; N, 9.27. Found: C, 55.36; H, 3.65; N, 9.04.

*5.1.2.1.7. (Z)-4-(3-Oxo-3-(2-oxo-2H-chromen-3-yl) prop-1-enylamino)-N-(1-phenyl-1H-pyraz-ol-5-yl) benzenesulfonamide **9**.* Yield, 89%; m.p. 203.0 °C. IR: 3226 (NH), 3031 (arom.), 2926, 2863 (aliph.), 1718, 1654 (2CO), 1609 (CN), 1334, 1152 (SO_2). ^{1}H-NMR: 5.8, 6.7 [2d, 2H, CH═CH, J = 8.4 Hz], 6.9–8.5 [m, 15H, Ar–H], 8.7 [s, 1H, CH chromene], 10.6 [s, 1H, SO_2NH], 12.0 [s, 1H, NH]. ^{13}C-NMR: 98.7, 106.7, 115.8 (2), 116.4 (2), 124.7 (2), 125.2, 126.5 (2), 129.1 (3), 129.2, 130.5 (2), 140.0 (3), 146.0 (3), 154.6 (2), 158.6, 185.0. MS *m*/*z* (%): 512 (M^+) (5.26), 142 (100). Anal. Calcd. for $C_{27}H_{20}N_4O_5S$ (512.54): C, 63.27; H, 3.93; N, 10.93. Found: C, 62.91; H, 3.66; N, 11.36.

*5.1.2.1.8. (Z)-N-(5-Methyl-1,3,4-thiadiazol-2-yl)-4-(3-oxo-3-(2-oxo-2H-chromen-3-yl) prop-1-enylamino) benzenesulfonamide **10**.* Yield, 77%; m.p. 260.1 °C. IR: 3421, 3357 (NH), 3067 (arom.), 2932, 2836, (aliph.), 1733, 1685 (2CO), 1613 (CN), 1358, 1188 (SO_2). ^{1}H-NMR: 2.6 [s, 3H, CH_3], 6.5, 6.7 [2d, 2H, CH═CH, J = 8.5 Hz]. 7.2–8.5 [m, 8H, Ar–H], 8.7 [s, 1H, CH chromene], 10.5 [s, 1H, SO_2NH], 12.0 [s, 1H, NH]. ^{13}C-NMR: 16.4, 98.3, 112.4 (2), 115.8, 116.4, 125.2, 126.5, 128.0, 128.1, 130.5 (2), 134.0, 144.5, 145.9, 146.2, 154.6, 154.7, 159.3, 168.2, 184.6. MS *m*/*z* (%): 468 (M^+) (12.36), 91 (100). Anal. Calcd. for $C_{21}H_{16}N_4O_5S_2$ (468.51): C, 53.84; H, 3.44; N, 11.96. Found: C, 53.49; H, 3.12; N, 12.31.

*5.1.2.1.9. (Z)-4-(3-Oxo-3-(2-oxo-2H-chromen-3-yl) prop-1-enylamino)-N-(pyridin-2-yl) benze-nesulfonamide **11**.* Yield, 77%; m.p. 274.2 °C. IR: 3302, 3290 (NH), 3101 (arom.), 2931, 2889, 2819 (aliph.), 1718, 1668 (2CO), 1608 (CN), 1386, 1184 (SO_2). ^{1}H-NMR: 6.5, 6.9 [2d, 2H, CH═CH, J = 8.6 Hz], 7.0–8.5 [m, 12H, Ar–H], 8.7 [s, 1H, CH chromene], 10.5 [s, 1H, SO_2NH], 12.0 [s, 1H, NH]. ^{13}C-NMR: 98.1, 108.4, 112.7 (2), 115.7 (2), 116.6, 124.7, 128.9 (2), 129.1 (3), 137.0 (2), 144.8, 145.4, 147.6, 154.3 (2), 155.7 (2), 184.7. MS *m*/*z* (%): 447 (M^+) (11.32), 231 (100). Anal. Calcd. for $C_{23}H_{17}N_3O_5S$ (447.46): C, 61.74; H, 3.83; N, 9.39. Found: C, 61.38; H, 4.13; N, 9.10.

*5.1.2.1.10. (Z)-4-(3-Oxo-3-(2-oxo-2H-chromen-3-yl) prop-1-enylamino)-N-(pyrimidin-2-yl)-benzenesulfonamide **12**.* Yield, 80%; m.p. 279.9 °C. IR: 3410, 3261 (NH), 3080 (arom.), 2941, 2872 (aliph.), 1716, 1653 (2CO), 1608 (CN), 1338, 1163 (SO_2). ^{1}H-NMR: 6.0, 6.8 [2d, 2H, CH═CH, J = 8.4 Hz], 6.9–8.5 [m, 11H, Ar–H], 8.7 [s, 1H, CH chromene], 10.4 [s, 1H, SO_2NH], 12.0 [s, 1H, NH]. ^{13}C-NMR: 95.2, 112.6 (2), 115.9 (2), 116.7, 125.7 (2), 130.1 (2), 130.2 (2), 133.7, 144.1, 145.8, 153.5 (2), 157.7 (2), 158.7, 173.7, 182.6. MS *m*/*z* (%): 448 (M^+) (5.72), 157 (100). Anal. Calcd. for $C_{22}H_{16}N_4O_5S$ (448.45): C, 58.92; H, 3.60; N, 12.49. Found: C, 58.57; H, 3.93; N, 12.18.

*5.1.2.1.11. (Z)-N-(4-Methylpyrimidin-2-yl)-4-(3-oxo-3-(2-oxo-2H-chromen-3-yl) prop-1-enyla-mino) benzenesulfonamide **13**.* Yield, 92%; m.p. 241.5 °C. IR: 3481, 3376 (NH), 3037 (arom.), 2912, 2876 (aliph.), 1718, 1654 (2CO), 1596 (CN), 1370, 1186 (SO_2). ^{1}H-NMR: 2.3 [s, 3H, CH_3], 6.6, 6.8 [2d, 2H, CH═CH, J = 8.5 Hz], 6.9–8.5 [m, 10H, Ar–H], 8.7 [s, 1H, CH chromene], 10.5 [s, 1H, SO_2NH], 12.0 [s, 1H, NH]. ^{13}C-NMR: 23.8, 104.0, 112.4, 115.2 (2), 116.4, 119.1, 125.2, 126.5, 127.6, 128.7, 130.3 (2), 134.0, 145.0, 146.9, 153.4, 154.6 (2), 157.4, 168.4, 172.5 (2). MS *m*/*z* (%): 462 (M^+) (8.47), 107 (100). Anal. Calcd. for $C_{23}H_{18}N_4O_5S$ (462.48): C, 59.73; H, 3.92; N, 12.11. Found: C, 59.44; H, 4.30; N, 12.46.

*5.1.2.1.12. (Z)-N-(4,6-Dimethylpyrimidin-2-yl)-4-(3-oxo-3-(2-oxo-2H-chromen-3-yl) prop-1-enylamino) benzenesulfonamide **14**.* Yield, 88%; m.p. 185.3 °C. IR: 3421, 3296, (NH), 3100 (arom.), 2966, 2851 (aliph.), 1718, 1700 (2CO), 1597 (CN), 1381, 1159 (SO_2). ^{1}H-NMR: 2.2 [s, 6H, $2CH_3$], 6.5, 6.8 [2d, 2H, CH═CH, J = 8.5 Hz], 6.9–8.0 [m, 9H, Ar–H], 8.5 [s, 1H, CH chromene], 10.4 [s, 1H, SO_2NH], 12.0 [s, 1H, NH]. ^{13}C-NMR: 21.5 (2), 103.8, 112.3, 114.0 (2), 115.1, 116.4, 125.2, 126.4, 127.3, 128.9, 130.4 (2), 133.8, 144.4, 146.0, 154.6, 154.7, 156.7,

167.8 (2), 172.5 (2). MS *m/z* (%): 476 (M^+) (9.17), 121 (100). Anal. Calcd. for $C_{24}H_{20}N_4O_5S$ (476.50): C, 60.49; H, 4.23; N, 11.76. Found: C, 60.14; H, 5.51; N, 11.41.

5.1.2.1.13. (Z)-N-(2,6-Dimethylpyrimidin-2-yl)-4-(3-oxo-3-(2-oxo-2H-chromen-3-yl) prop-1-enylamino) benzenesulfonamide ***15***. Yield, 82%; m.p. 215.1 °C. IR: 3409, 3372 (NH), 3090 (arom.), 2923, 2839 (aliph.), 1718, 1684 (2CO), 1610 (CN), 1371, 1187 (SO_2). ^{1}H-NMR: 2.2, 2.3 [s, 6H, $2CH_3$], 6.5, 6.9 [2d, 2H, CH═CH, J = 8.6 Hz], 7.1–8.5 [m, 9H, Ar–H], 8.7 [s, 1H, CH chromene], 10.4 [s, 1H, SO_2NH], 12.0 [s, 1H, NH]. ^{13}C-NMR: 19.0, 21.5, 95.3, 105.7, 115.5 (2), 116.4, 119.1, 127.6 (2), 129.1 (2), 130.5 (2), 131.8, 147.2 (2), 154.6 (2), 159.3 (2), 159.6, 166.7, 172.7. MS *m/z* (%): MS *m/z* (%): 476 (M^+) (11.32), 106 (100). Anal. Calcd. for $C_{24}H_{20}N_4O_5S$ (476.50): C, 60.49; H, 4.23; N, 11.76. Found: C, 60.85; H, 3.97; N, 12.12.

5.1.2.1.14. (Z)-N-(5-Methoxypyrimidin-2-yl)-4-(3-oxo-3-(2-oxo-2H-chromen-3-yl) prop-1-enyl-amino) benzenesulfonamide ***16***. Yield, 84%; m.p. 255.9 °C. IR: 3419, 3216, (NH), 3031 (arom.), 2909, 2801 (aliph.), 1718, 1654 (2CO), 1610 (CN), 1334, 1152 (SO_2). ^{1}H-NMR: 3.8 [s, 3H, OCH_3], 6.6, 6.9 [2d, 2H, CH═CH, J = 8.4 Hz], 7.0–8.5 [m, 10H, Ar–H], 8.6 [s, 1H, CH chromene], 10.4 [s, 1H, SO_2NH], 12.0 [s, 1H, NH]. ^{13}C-NMR: 56.7, 104.0, 112.6 (2), 115.5, 119.1, 125.2, 126.5, 127.9, 128.4, 129.8 (2), 133.6, 144.5 (2), 144.9, 145.1, 146.0, 151.3, 154.6, 159.3 (2), 172.5. MS *m/z* (%): 478 (M^+) (16.07), 142 (100). Anal. Calcd. for $C_{23}H_{18}N_4O_6S$ (478.48): C, 57.73; H, 3.79; N, 11.71. Found: C, 57.46; H, 4.07; N, 12.05.

5.1.2.1.15. (Z)-N-(2,6-Dimethoxypyrimidin-4-yl)-4-(3-oxo-3-(2-oxo-2H-chromen-3-yl) prop-1-enylamino) benzenesulfonamide ***17***. Yield, 80%; m.p. 215.0 °C. IR: 3421, 3219 (NH), 3100 (arom.), 2941, 2870 (aliph.), 1710, 1654 (2CO), 1609 (CN), 1380, 1164 (SO_2). ^{1}H-NMR: 3.77, 3.79 [2s, 6H, $2OCH_3$], 5.9 [s, 1H, CH pyrimidine], 6.2, 6.8 [2d, 2H, CH═CH, J = 8.4 Hz], 6.9–8.6 [m, 8H, Ar–H], 8.7 [s, 1H, CH chromene], 10.6 [s, 1H, SO_2NH], 11.9 [s, 1H, NH]. ^{13}C-NMR: 55.0, 56.5, 85.0, 98.7, 109.9 (2), 115.7, 116.9, 125.1, 126.3, 128.1, 129.6, 130.7 (2), 133.9, 144.2, 146.0, 150.8, 154.6, 158.8, 159.2, 164.7, 172.5, 192.5. MS *m/z* (%): 508 (M^+) (13.57), 153 (100). Anal. Calcd. for $C_{24}H_{20}N_4O_7S$ (508.50): C, 56.69; H, 3.96; N, 11.02. Found: C, 56.36; H, 3.65; N, 11.34.

5.1.2.1.16. (Z)-N-(5,6-Dimethoxypyrimidin-4-yl)-4-(3-oxo-3-(2-oxo-2H-chromen-3-yl) prop-1-enylamino) benzenesulfonamide ***18***. Yield, 78%; m.p. 209.9 °C. IR: 3356, 3212 (NH), 3078 (arom.), 2951, 2836 (aliph.), 1718, 1646 (2CO), 1593 (CN), 1340, 1161 (SO_2). ^{1}H-NMR: 3.7, 3. 9 [2s, 6H, $2OCH_3$], 6.5, 6.9 [2d, 2H, CH═CH, J = 8.6 Hz], 7.1–8.5 [m, 9H, Ar–H], 8.6 [s, 1H, CH chromene], 10.6 [s, 1H, SO_2NH], 12.0 [s, 1H, NH]. ^{13}C-NMR: 54.4, 60.6, 98.6, 115.4 (2), 116.4, 118.9, 125.1, 126.4, 127.7, 129.9, 130.5 (2), 130.8, 133.9, 144.0, 146.9, 150.9, 154.6, 154.7, 158.9, 159.3, 162.0, 184.6. MS *m/z* (%): 508 (M^+) (11.22), 151 (100). Anal. Calcd. for $C_{24}H_{20}N_4O_7S$ (508.50): C, 56.69; H, 3.96; N, 11. 02. Found: C, 56.92; H, 4.32; N, 11.28.

5.1.2.1.17. (Z)-N-(1H-Indazol-6-yl)-4- (3-oxo-3-(2-oxo-2H-chromen-3-yl) prop-1-enylamino) be-nzenesulfonamide ***19***. Yield, 81%; m.p. 198.7 °C. IR: 3367, 3317 (NH), 3100 (arom.), 2944, 2861 (aliph.), 1718, 1653 (2CO), 1609 (CN), 1388, 1154 (SO_2). ^{1}H-NMR: 6.5, 6.8 [2d, 2H, CH═CH, J = 8.5 Hz], 6.9–7.9 [m, 11H, Ar–H], 8.1 [s, 1H, CH indazole], 8.5 [s, 1H, CH chromene], 10.3 [s, 1H, SO_2NH], 11.9 [s, 1H, NH], 12.9 [s, 1H, NH indazole], ^{13}C-NMR: 88.6, 100.4, 104.1, 115.3 (2), 115.8, 116.4, 117.0, 119.1, 120.2, 125.1, 126.4, 127.8, 128.4, 130.8 (2), 133.8, 140.6, 144.0, 145.0, 146.9, 154.6, 154.7, 158.9, 185.5. MS *m/z* (%): 486 (M^+) (4.88), 169 (100). Anal. Calcd. for $C_{25}H_{18}N_4O_5S$ (486.50): C, 61.72; H, 3.73; N, 11. 52. Found: C, 61.43; H, 4.01; N, 11.90.

5.1.2.1.18. (Z)-4-(3-Oxo-3-(2-oxo-2H-chromen-3-yl) prop-1-enylamino)-N-(quinoxalin-2-yl) benzenesulfonamide ***20***. Yield, 78%; m.p. 250.0 °C. IR: 3408, 3250 (NH), 3069 (arom.), 2961, 2844 (aliph.), 1729, 1639 (2CO), 1609 (CN), 1351, 1161 (SO_2). ^{1}H-NMR: 6.4, 6.9 [2d, 2H, CH═CH, J = 8.5 Hz], 7.2–8.5 [m, 13H, Ar–H], 8.6 [s, 1H, CH chromene], 10.5 [s, 1H, SO_2NH], 11.9 [s, 1H, NH]. ^{13}C-NMR: 98.6, 112.7 (2), 115.5, 118.9, 125.1, 126.3, 127.3, 129.1 (2), 130.1 (2), 130.5, 130.7 (2), 133.1, 134.3, 134.8, 138.1, 144.2, 146.0, 154.6, 154.8, 159.2, 172.5, 184.5. MS *m/z* (%): 498 (M^+) (9.76), 128 (100). Anal. Calcd. for $C_{26}H_{18}N_4O_5S$ (498.51): C, 62.64; H, 3.64; N, 11. 24. Found: C, 62.26; H, 3.30; N, 10.88.

5.1.2.1.19. (Z)-3-(3-(4-(4-Aminophenylsulfonyl) phenylamino) acryloyl)-2H-chromen-2-one ***21***. A mixture of **2** (1.88 g, 0.01 mol) and dapsone (2.48 g, 0.01 mol) in absolute ethanol (10 mL) and glacial acetic acid (5 mL) was refluxed for 11 h. The obtained solid while hot was recrystallized from dioxane to give **21**.

Yield, 75%; m.p. 249.9 °C. IR: 3431, 3413, 3396 (NH_2, NH), 3079 (arom.), 2967, 2881 (aliph.), 1718, 1654 (2CO), 1363, 1181 (SO_2). ^{1}H-NMR: 6.1, 6.8 [2d, 2H, CH═CH, J = 8.6 Hz], 6.2 [s, 2H, NH_2], 6.9–8.5 [m, 12H, Ar–H], 8.6 [s, 1H, CH chromene], 10.8 [s, 1H, NH]. ^{13}C-NMR: 91.6, 112.9 (2), 113.1 (2), 116.4, 117.6, 125.2, 128.9 (2), 130.6 (4), 131.8 (2), 136.1, 143.6, 145.8, 155.3 (3), 159.6, 172.4. MS *m/z* (%): 446 (M^+) (2.98), 92 (100). Anal. Calcd. for $C_{24}H_{18}N_2O_5S$ (446.48): C, 64.56; H, 4.06; N, 6.27. Found: C, 64.31; H, 4.38; N, 6.00.

5.1.2.1.20. (2Z,2′Z)-3,3′-(4,4′-sulfonylbis(4,1-phenylene)bis(azanediyl))bis(4-(3-oxo-3-(2-oxo-2H-chromen-3-yl)prop-2-en-1-one ***22***. A mixture of **2** (3.76 g, 0.02 mol) and dapson (2.48 g, 0.01 mol) in absolute ethanol (10 mL) and glacial acetic acid (5 mL) was refluxed for 12 h. The obtained solid while hot was recrystallized from acetic acid to give **22**.

Yield, 73%; m.p. 221.6 °C. IR: 3421, 3366 (NH), 3091 (arom.), 2964, 2871 (aliph.), 1718, 1636 (4CO), 1361, 1181 (SO_2). ^{1}HNMR: 6.2, 6.6 [2d, 4H, 2CH═CH, J = 8.5 Hz], 6.9–8.5 [m, 16H, Ar–H], 8.7 [s, 2H, 2CH chromene], 10.9 [s, 2H, 2NH]. ^{13}C NMR: 96.7 (2), 112.8 (4), 116.4 (2), 118.6 (2), 125.6 (2), 126.7 (4), 130.6 (4), 133.7 (2), 134.2 (2), 141.6 (2), 144.7 (2), 151.4 (2), 153.6 (2), 159.6 (2), 172.5 (2). MS *m/z* (%): 644 (M^+) (37.19), 303 (100). Anal. Calcd. for $C_{36}H_{24}N_2O_8S$ (644.65): C, 67.07; H, 3.75; N, 4.35. Found: C, 67.38; H, 3.41; N, 4.04.

5.2. Biological evaluation

5.2.1. In-vitro anticancer evaluation

The cytotoxic activity *in vitro* of the novel synthesized compounds was measured in T47D breast cancer cells and 184A1 normal breast cells using the sulforhodamine B stain (SRB) assay and the method of Skehan et al. [19]. The human breast cancer cell line T47D (obtained from National Cancer Institute, Cairo, Egypt) and the 184A1 normal breast cells (obtained from VACSERA, Cairo, Egypt) were maintained at 37 °C in 5% CO_2 as sub confluent monolayers in 80 cm^3 culture flasks (Nunclon) and were subculture once or twice weekly in RPMI 1640 (Invitrogen/Life Technologies) supplemented with 10% heat inactivated fetal bovine serum FBS (Hyclone), and 1% penicillin-streptomycin-amphoterecin-B. Passage levels were in the range of 5–20 according to the original receipt. Cells were harvested from exponential phase cultures by trypsinisation, counted and plated in 96-well flat bottomed microliter plates (Greiner Labortechnik, Germany) (100 μL cell suspension containing 10^4 cells per well). Following plating and a 24-h recovery to allow cells to resume exponential growth, 100 μL culture medium or culture medium containing the drug was added to the wells. Test compounds were dissolved in DMSO as a 0.1 mol L^{-1} stock solution (the final concentration of DMSO in culture medium was less than 0.1%) and diluted with phosphate buffered saline (PBS) to from 10 μmol L^{-1} stock solution. Different concentrations of each test compound (5, 12, 25 and 50 μmol L^{-1}) were added to the cell monolayer. Triplicate wells were prepared for each individual dose. Monolayer cells were incubated with the compound(s) for 48 h at 37 °C and in an atmosphere of 5% CO_2. Forty eight hours after drug addition, cells were fixed with 50% trichloroacetic acid at 4 °C (50 μL/well) for 1 h, washed with 1%

acetic acid and stained for 30 min with 50 μL of 0.4% (m/V) SRB dissolved in 1% acetic acid. Excess unbound dye was removed by four washes with 1% acetic acid and attached stain was recovered with Tris-EDTA buffer. Color intensity was measured using an enzyme-linked immunosorbent assay ELISA reader. Optical density was read at 540 nm [19]. The relation between the surviving fraction and drug concentration was plotted to get the survival curve for the breast cancer cell line (T47D) after specified time and the dose-response curves were analyzed using the E_{max} model (Eq. (1)) [23]

$$\%\ \text{Cell viability} = (100 - R) \times \left(1 - \frac{[D]^m}{K_d^m + [D]^m}\right) + R \quad (1)$$

Where R is the residual unaffected fraction (resistance fraction); [D] is the drug concentration used, K_d is the drug concentration that produces 50% reduction of the maximum inhibition rate, and m is a Hill-type coefficient. IC_{50} was defined as the drug concentration that produces 50% reduction in the color intensity compared to that of the control (i.e., $K_d = IC_{50}$ when $R = 0$ and $E_{max} = 100 - R$). The results are shown in Table 1.

5.2.2. Effect of the synthesized compounds on aromatase activity

T47D cells were cultured using RPMI 1640 (Invitrogen/Life Technologies) supplemented with 10% FBS (Hyclone), and 1% penicillin-streptomycin. The aromatase activity was tested using Aromatase (Cytochrome P450 19A1) human ELISA Kit (Biovision, Milpitas, CA 95035, USA) (Catalog #K3599-100). The cells were seeded at a density (1.2–1.8 × 10,000 cells/well) in a volume of 100 μl complete growth medium +100 μL of the tested compound per well in a 96-well plate for 24 h before the enzyme assay for aromatase according to the manufacturer's instructions.

5.2.3. Determination of the aromatase IC_{50}

T47D cells were treated with serial dilutions of the selected potent compounds for 24 h and then the aromatase activity was determined using Aromatase (Cytochrome P450 19A1) human ELISA Kit (Biovision, Milpitas, CA 95035, USA) (Catalog #K3599-100) according to the manufacturer's instructions.

5.2.4. Determination of the active caspase-3

To determine the effect of the synthesized compounds on apoptosis, the active caspase-3 level was measured by using Quantikine -Human active Caspase-3 Immunoassay (R&D Systems, Inc. Minneapolis, USA) according to the manufacturer protocol. Briefly, after washing the cells with PBS, the cells were collected and lysed by adding it to the extraction buffer containing protease inhibitors (1 mL per 1×10^7 cells) then the lysate was diluted immediately prior to the assay. At the end of the assay the optical density of each well was determined within 30 min using a microplate reader set at 450 nm.

5.2.5. Determination of caspase-8 & caspase-9

Cells were grown in RPMI 1640 containing 10% fetal bovine serum at 37 °C, stimulated with the compounds to be tested for caspases 8 & 9, using human caspase-8 ELISA kit **(EIA-4863)** and human caspase-9 ELISA kit **DRG® Caspase-9 (EIA-4860)** (**DRG International Inc., USA**). Cells were lysed with cell extraction buffer. This lysate was diluted in standard diluent buffer over the range of the assay and measured for human caspase-8 & caspase-9 content, separately. For each assay the cells were plated in a density of 1.2–1.8 × 10,000 cells/well in a volume of 100 μl complete growth medium +100 μL of the tested compound per well in a 96-well plate for 48 h before the enzyme assay for caspase-8 & 9 according to the manufacturer's protocol. Finally, the absorbance of each microwell was read using a microplate reader set at 450 nm.

5.2.6. RNA extraction, real time PCR analysis and quantification of gene expression

The gene expression of Bax, Bcl-2, Bcl-xl was assessed by total RNA extraction from cells using RNeasy Mini Kit® (Qiagen Inc. Valencia, CA, USA). cDNA library was constructed from different treatments using High-Capacity cDNA Reverse Transcription Kit (Applied Biosystems, Foster City, CA). The archived cDNA libraries were then subjected to quantitative real time PCR reactions [24] using cyber green fluorophore (Fermentas Inc., Glen Burnie, MD, USA). Primer sequences for each gene were as follows: Bcl-2 forward primer GGG-TAC-GAT-AAC-CGG-GAG-AT and reverse primer CTG-AAG-AGC-TCC-TCC-ACC-AC; Bax forward primer TCT-GAC-GGC-AAC-TTC-AAC-TG and reverse primer TGG-GTG-TCC-CAA-AGT-AGG-AG; Bcl-xl forward primer GGC GGA TTT GAA TCT CTT TCT C and reverse primer TTA TAA TAG GGA TGG GCT CAA CC; GAPDH was used as reference housekeeping gene with forward primer TGC-ACC-ACC-AAC-TGC-TTA-G and reverse primer GAT-GCA-GGG-ATG-ATG-TTC [21].

5.2.7. Analysis of cell cycle distribution

To determine the effect of compounds **8 & 16** on the cell cycle distribution T47D cell line; cell cycle analysis was performed using the CycleTEST™ PLUS DNA Reagent Kit (Becton Dickinson Immunocytometry Systems, San Jose, California, USA). Control cells with known DNA content (PBMCs) were used as a reference point for determining the DI (DNA Index) for the test samples. The cells were stained with propodium iodide stain following the procedure provided by the kit and then run on the DNA cytometer. Cell cycle distribution was calculated using CELLQUEST software (Becton Dickinson Immunocytometry Systems, San Jose, California, USA).

5.3. Molecular docking

Molecular docking was performed to elucidate interactions of investigated compounds toward its target protein namely the aromatase enzyme. Initially, the crystal structure of the human placental aromatase (cytochrome P450, member 19A1) co-crystallized with the androstanedione (ASD) substrate was retrieved from the Protein Data Bank (PDB ID: 3EQM). Docking study was performed using Accelerys software (Discovery Studio 2.5) in the computer drug design lab in pharmaceutical chemistry department, faculty of pharmacy, Ain Shams University. The protein was prepared for docking process according to the standard protein preparation procedure integrated in Accelry's discovery studio 2.5 and prepared by prepares protein protocol. Androstandione, lead compound (hit 1) and our ligands were drawn as a database and prepared by prepare ligand protocol to generate 3D structure and refined using CHARMM force field with full potential. Docking simulations were run using CDOCKER protocol where maximum bad orientations was 800 and orientation vdW energy threshold was 300. Simulated annealing simulation would be then carried out consisting of a heating phase 700 K with 2000 steps and a cooling phase back to 5000 steps. The binding energy was calculated as a score to rank the docking poses. The top 10 docking poses would were finally saved. Docking poses were ranked according to their CDOCKER interaction energy, and the top pose was chosen for analysis of interactions for each compound.

Acknowledgment

The authors would like to extend their sincere appreciation to the Deanship of Scientific Research at King Saud University for its

funding of this research through the Research Group Project No. **RGP-302**.

Appendix A. Supplementary data

Supplementary data related to this article can be found at http://dx.doi.org/10.1016/j.ejmech.2016.10.020.

References

[1] T. Sørlie, Molecular portraits of breast cancer: tumour subtypes as distinct disease entities, Eur. J. Cancer 40 (2004) 2667–2675.
[2] R. Nahta, F.J. Esteva, Herceptin: mechanisms of action and resistance, Cancer Lett. 232 (2006) 123–138.
[3] A. Jemal, F. Bray, M.M. Center, J. Ferlay, E. Ward, D. Forman, Global cancer statistics, Cancer J. Clin. 61 (2011) 69–90.
[4] M.R. Yadav, M.A. Barmade, R.S. Tamboli, P.R. Murumkar, Developing steroidal aromatase inhibitors-an effective armament to win the battle against breast cancer, Euro. J. Med. Chem. 105 (2015) 1–38.
[5] M.D. Matteo, A. Ammazzalorso, F. Andreoli, I. Caffa, B.D. Fillippis, M. Fantacuzzi, L. Giampeitro, C. Maccallini, M.D. Parenti, D. Soncini, A.D. Rio, R. Amoroso, Synthesis and biological characterization of 3-(imidazol-1-ylmethyl) piperidine sulfonamides as aromatase inhibitors, Bioorg. Med. Chem. Lett. 26 (2016) 3192–3194.
[6] I. Ahmad, Shagufta, Recent developments in steroidal and nonsteroidal aromatase inhibitors for the chemoprevention of estrogen-dependent breast cancer, Euro. J. Med. Chem. 102 (2015) 375–386.
[7] C. Ouellet, R. Maltais, É. Ouellet, X. Barbeau, P. Lagüe, D. Poirier, Discovery of a sulfamate-based steroid sulfatase inhibitor with intrinsic selective estrogen receptor modulator properties, Euro. J. Med. Chem. 119 (2016) 169–182.
[8] J. Narashimamurthy, A.R. Rao, G.N. Sastry, Aromatase inhibitors: a new paradigm in breast cancer treatment, Curr. Med. Chem. Anticancer Agents 4 (2004) 523–534.
[9] J.K. Litton, B.K. Arun, P.H. Brown, G.N. Hortobagyi, Aromatase inhibitors and breast cancer prevention, Expert Opin. Pharmacother. 13 (2012) 325–331.
[10] R. Pingaew, V. Prachayasittikul, P. Mandi, C. Nantasenamat, S. Prachayasittikul, S. Ruchirawat, V. Prachayasittikul, Synthesis and molecular docking of 1,2,3-triazole-based sulfonamides as aromatase inhibitors, Bioorg. Med. Chem. 23 (2015) 3472–3480.
[11] J.Z. Ji, K.J. Lao, J. Hu, T. Pang, Z.Z. Jiang, H.L. Yuan, Discovery of novel aromatase inhibitors using a homogeneous time-resolved fluorescence assay, Acta Pharm. Sin. 35 (8) (2014) 1082–1092.
[12] M. Lanzino, P. Maris, R. Sirianni, I. Barone, I. Casaburi, A. Chimento, C. Giordano, C. Morelli, D. Sisci, P. Rizza, D. Bonofiglio, S. Catalano, S. Andò, DAX-1, as an androgen-target gene, inhibits aromatase expression: a novel mechanism blocking estrogen-dependent breast cancer cell proliferation, Cell Death Dis. 4 (2013) 724.
[13] D.C. Wallace, Mitochondria and cancer, Nat. Rev. Cancer 12 (2012) 685–698.
[14] B. Yu, S.Q. Wang, P.P. Qi, D.X. Yang, K. Tang, H.M. Liu, Design and synthesis of isatin/triazole conjugates that induce apoptosis and inhibit migration of MGC-803 cells, Euro. J. Med. Chem. 124 (2016) 350–360.
[15] Z.R. Wu, J. Liu, J.Y. Li, L.F. Zheng, Y. Li, X. Wang, Q.J. Xie, A.X. Wang, Y.H. Li, R.H. Liu, H.Y. Li, Synthesis and biological evaluation of hydroxycinnamic acid hydrazide derivatives as inducer of caspase-3, Euro. J. Med. Chem. 85 (2014) 778–783.
[16] Y. Tsujimoto, Cell death regulation by the Bcl-2 protein family in the mitochondria, J. Cell Physiol. 195 (2003) 158–167.
[17] G.M. Callagy, M.J. Webber, P.D. Pharoah, C. Caldas, Meta-analysis confirms BCL2 is an independent prognostic marker in breast cancer, BMC Cancer 8 (2008) 153–162.
[18] T.J. McDonnell, S.J. Korsmeyer, Progression from lymphoid hyperplasia to high-grade malignant lymphoma in mice transgenic for the t (14; 18), Nature 349 (1991) 254–256.
[19] H. Zhu, J. Zhang, N. Xue, Y. Hu, B. Yang, Q. He, Novel combretastatin A-4 derivative XN0502 induces cell cycle arrest and apoptosis in A549 cells, Invest. New Drugs 28 (2010) 493–501.
[20] N.M. Weir, K. Selvendiran, V.K. Kutala, L. Tong, S. Vishwanath, M. Rajaram, S. Tridandapani, S. Anant, P. Kuppusamy, Curcumin induces G2/M arrest and apoptosis in cisplatin-resistant human ovarian cancer cells by modulating Akt and p38 MAPK, Cancer Biol. Ther. 6 (2007) 178–184.
[21] (a) K.T. Chan, F.Y. Meng, Q. Li, C.Y. Ho, T.S. Lam, Y. To, W.H. Lee, M. Li, K.H. Chu, M. Toh, Cucurbitacin B induces apoptosis and S phase cell cycle arrest in BEL-7402 human hepatocellular carcinoma cells and is effective via oral administration, Cancer Lett. 294 (2010) 118–124;
(b) J.K. Shen, H.P. Du, M. Yang, Y.G. Wang, J. Jin, Casticin induces leukemic cell death through apoptosis and mitotic catastrophe, Ann. Hematol. 88 (2009) 743–752.
[22] P. Skehan, R. Storeng, D. Scudiero, A. Monks, J. McMahon, D. Vistica, J.T. Warren, H. Bokesch, S. Kenney, M.R. Boyd, New colorimetric cytotoxicity assay for anticancer-drug screening, J. Natl. Cancer Inst. 82 (1990) 1107–1112.
[23] A.M. Mahmoud, A.M. Al-Abd, D.A. Lightfoot, H.A. El-Shemy, Anti-cancer characteristics of mevinolin against three different solid tumor cell lines was not solely p53-dependent, J. Enzyme Inhib. Med. Chem. 27 (2012) 673–679.
[24] M.C. Longo, M.S. Berninger, J.L. Hartley, Use of uracil DNA glycosylase to control carry-over contamination in polymerase chain reactions, Gene 93 (1990) 125–128.